



G&G

Micro-World

Editor: Nathan Renfro

Contributing Editors: John I. Koivula and Tyler Smith

Shrinkage Cracks in Fire Agate

Over the last few years, the author has encountered numerous examples of fire agate (a variety of quartz chalcedony) displaying a random weblike pattern, including a parcel of cabochons from Mexico purchased at the 2023 Tucson gem shows. Fire agates typically show a botryoidal structure reminiscent of a cluster of grapes, so this unusual pattern was quite noteworthy.

Microscopic examination of the cabochons revealed that the pattern was most likely the result of shrinkage cracks caused by desiccation. This drying out created a volume reduction that pulled apart the silica material during formation of the fire agate, producing a pattern of irregular separations that were later infilled by a secondary generation of chalcedony, which then preserved the pattern (figure 1). These shrinkage cracks stand out in high contrast to the host chalcedony as interruptions in the iridescent phenomenon that result from broken layers of goethite where shrinkage occurred. While not particularly common, shrinkage cracks in fire agate create a unique pattern in this colorful gem material.

*Nathan Renfro
GIA, Carlsbad*

About the banner: This goldstone glass contains numerous copper crystals that are responsible for the aventurescent phenomenon seen in this manufactured material. Photomicrograph by Nathan Renfro; field of view 2.18 mm.

GEMS & GEMOLOGY, VOL. 60, No. 1, pp. 74–82.

© 2024 Gemological Institute of America

Hairlike Inclusions in Benitoite

The authors recently examined a 3.55 ct benitoite that featured whitish hairlike inclusions throughout the stone (figure 2). The inclusions were too thin to be identified by Raman spectroscopy.

Gem-quality benitoite has been extracted from a single mine in California and is reported to occur with natrolite gangue in altered blueschist within serpentinite. Minerals found within benitoite include actinolite-tremolite, aegirine-augite, diopside, serandite pseudomorphs, neptunite, jaquinite, albite, apatite, and djurleite (B.M. Laurs et al.,

Figure 1. This fire agate from Mexico displays an interesting weblike network of shrinkage cracks that were likely the result of desiccation during formation. Photomicrograph by Nathan Renfro; field of view 4.11 mm.

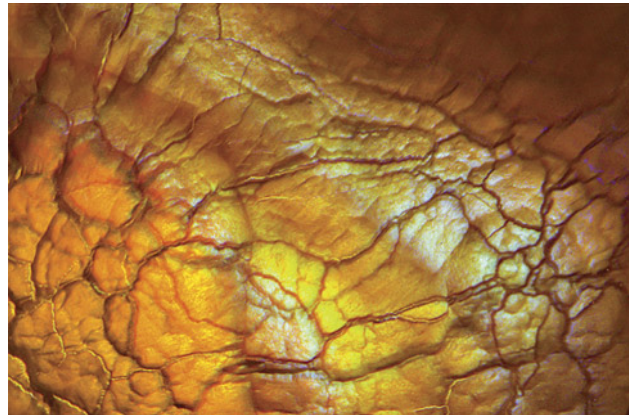




Figure 2. Whitish hairlike inclusions in a 3.55 ct faceted benitoite. Photomicrograph by Taku Okada; field of view 2.37 mm.

“Benitoite from the New Idria District, San Benito County, California,” Fall 1997 *G&G*, pp. 166–187). Therefore, the hairlike inclusions in this stone could be natrolite, chrysotile (white asbestos), or tremolite, which have whitish colors and acicular or fibrous crystal habits.

*Taku Okada and Yusuke Katsurada
GIA, Tokyo*

Stellate Cloud in Diamond

Impurity clouds in diamonds occur in a variety of forms such as scattered, planar, or patchy clouds. The author re-

Figure 3. This patchy cloud with an uneven distribution of pinpoints observed in a natural diamond appears to depict a celestial star. The image was captured in monochrome. Photomicrograph by Tejas Jhaveri; field of view 2.9 mm.

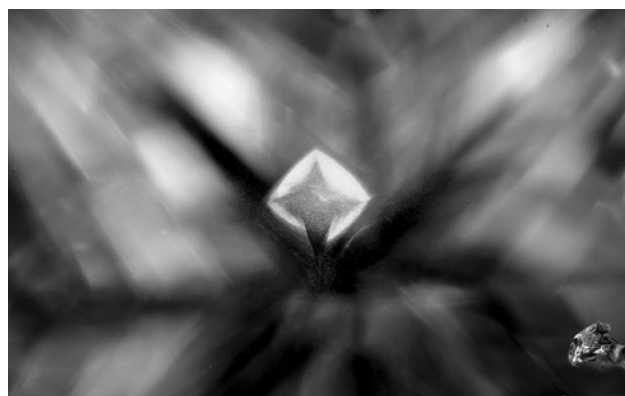


Figure 4. A collection of trigons on the pavilion surface of a round brilliant-cut diamond. Photomicrograph by Isabelle Corvin; field of view approximately 2.0 mm.

cently observed one such cloud with an unusual morphology in a 1.51 ct natural diamond with E color and SI₂ clarity (figure 3). This remarkable cluster of pinpoints took the form of a four-point star. This celestial inclusion is sure to be seen as a lucky charm.

*Tejas Jhaveri
GIA, Mumbai*

Trigon Party on a Diamond

Triangular-shaped markings known as trigons are common in natural diamond. These “birthmarks” formed during growth are signs of a diamond’s ancient origin deep within the earth. The trigons in figure 4 form a striking cluster on the faceted girdle and extend into two of the lower girdle facets of a 1.01 ct natural diamond. Even through the cutting and polishing process, these trigons remained on the surface.

Although trigons are not exceedingly rare, the assortment of this many trigons grouped together provides a remarkable portrait created by Mother Nature. The perfection of a diamond is on full display in the angles, luster, and alignment of each trigon.

*Isabelle Corvin
Olympia, Washington*

Iridescent Healed Fissures in Epidote

The author recently examined a 4.18 ct yellowish brown cushion-cut epidote. Under fiber-optic illumination, the stone revealed iridescent healed fissures (figure 5). Healed fissures are not uncommon in various gemstones. They are believed to result from a secondary fluid that facilitated the

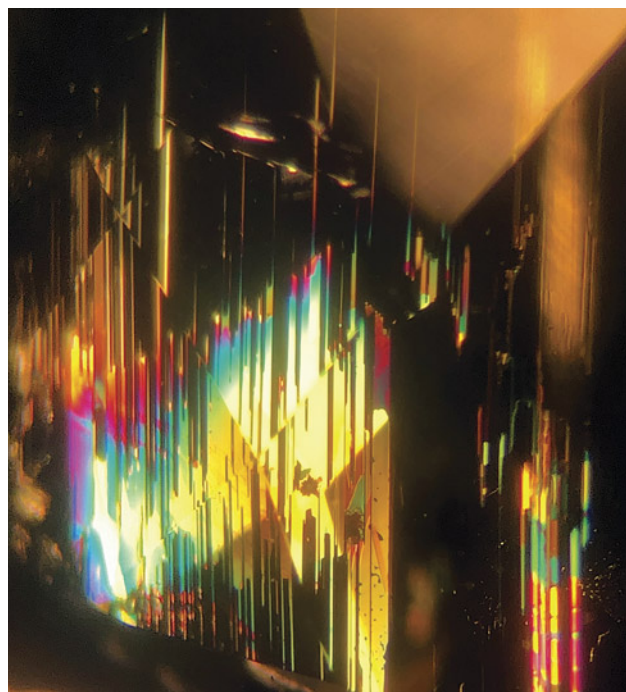


Figure 5. Iridescent healed fissures observed in a 4.18 ct faceted epidote. Photomicrograph by Tinh Xuan Nguyen; field of view 2.5 mm.

healing process of previously surface-reaching fractures. In the case of this epidote, the healed fissures resulted in a striking feature revealed when illuminated under the microscope.

Tinh Xuan Nguyen
PNJ Laboratory Company Limited
Ho Chi Minh City, Vietnam

Pink and Red Epidote in Quartz

We recently discovered very photogenic clusters of hot pink to red crystals as “firework” sprays (figure 6) in two transparent cabochons of rock crystal quartz. The cabochons weighed 5.47 ct and 11.18 ct and measured $15.85 \times 9.87 \times 5.92$ mm and $16.06 \times 11.49 \times 7.83$ mm, respectively (figure 7). These cabochons, which came from Sara Crystal in Shanghai, are thought to be from Chenzhou in China’s Hunan Province.

After performing gemological testing and optical microscopy, we thought the inclusions might be piemontite based on their behavior in polarized light and the monoclinic morphology of the individual terminated crystals. Because some of the pink crystals reached the surface of their polished hosts, we decided to analyze them using Raman microanalysis. The result was a close match for epidote, which was surprising since epidote is normally thought of as a dark brownish green mineral.

The results of chemical analysis using laser ablation–inductively coupled plasma–mass spectrometry were consistent with epidote, but with one additional element present: manganese, which caused the pink to red color in these microcrystals. We concluded that the inclusions were indeed epidote instead of piemontite, but pink to red epidote was something completely new to us.

Searching the literature for piemontite and epidote uncovered the following statement from Mindat.org, which seemed to explain the existence of these pink to red epidotes:

“Piemontite” has two different uses: Piemontite (*sensu stricto*) is the mineral species described here, but more commonly “piemontite” refers incorrectly to deep red colored, Mn^{3+} -bearing epidotes that are really varieties of the species epidote, and not strictly speaking piemontite. “Piemontites”

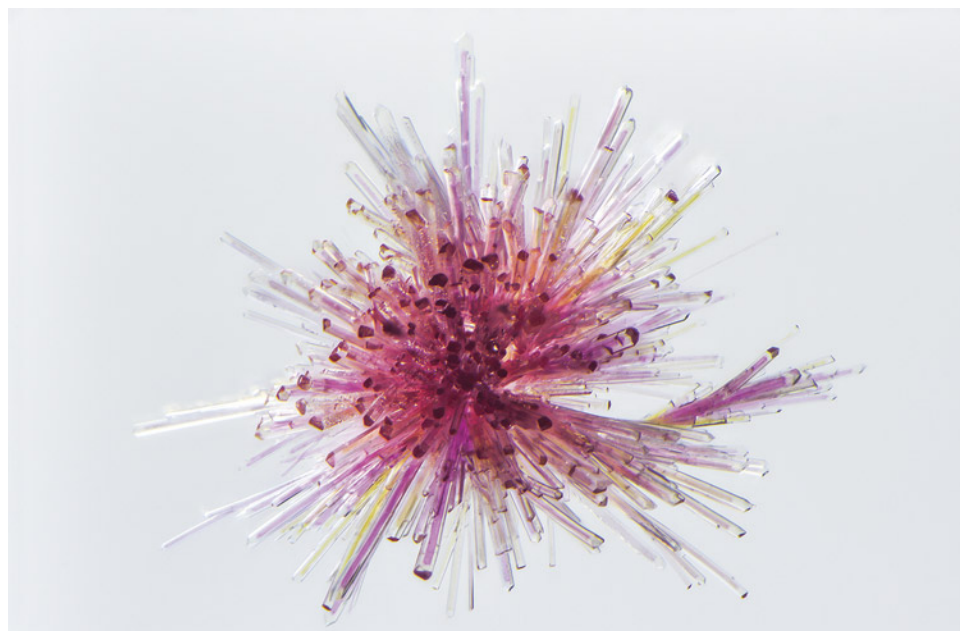


Figure 6. Bright pink to red epidote crystals as “firework” sprays were a surprising discovery in rock crystal quartz. Photomicrograph by Nathan Renfro; field of view 2.16 mm.

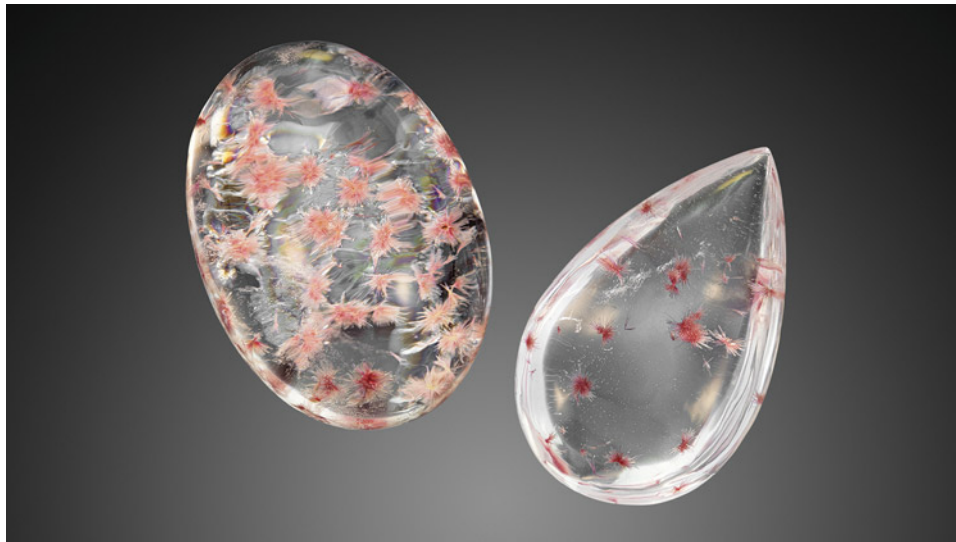


Figure 7. Weighing 11.18 ct (left) and 5.47 ct (right), these two rock crystal quartz cabochons play host to very unusual pink crystal sprays. Photo by Adriana Robinson.

rarely contain more than 40% of the piemontite molecule, so many “piemontites” in collections (and pictured here in Mindat) are really Mn-rich red varieties of epidote.

To our knowledge, this pink to red epidote-quartz inclusion-host association has not previously been reported.

*John I. Koivula, Nathan Renfro, and Maxwell Hain
GIA, Carlsbad*

Fluorite in Brazilian Alexandrite

The author recently examined a 1.25 ct transparent oval modified brilliant alexandrite. The stone possessed a single crystal inclusion in the shape of a perfect octahedron (figure 8). Raman analysis identified the crystal as fluorite (CaF_2), which supported the alexandrite host’s origin determination of Brazil.

Fluorite crystals are occasionally found in Brazilian alexandrite (Z. Sun et al., “Geographic origin determination

of alexandrite,” Winter 2019 *G&G*, pp. 660–681). However, they are often rounded in shape and rarely perfectly octahedral like the observed crystal here.

*Hikaru Sato
GIA, Tokyo*

Radial Limonite in Sapphire

Limonite, a composite of hydrated iron oxide minerals, is an inclusion commonly seen in corundum, usually as a thin yellow veil of epigenetic deposits within surface-reaching fractures. A unique example of this material is shown in figure 9, where limonite precipitated into a small fracture and formed in a radial fashion. When viewed under diffused reflected light, the inclusion displayed bright interference colors. The inclusion stands in sharp

Figure 8. An octahedral fluorite crystal in a 1.25 ct Brazilian alexandrite. Photomicrograph by Hikaru Sato; field of view 2.37 mm.



Figure 9. Radial limonite within a surface-reaching fracture of a violet sapphire shows bright interference colors when viewed under diffused reflected light. Photomicrograph by Nathan Renfro; field of view 1.44 mm.





Figure 10. A parasite channel with a surface opening and finer branch-like etch channels in a natural saltwater pearl. Photomicrograph by Emiko Yazawa; field of view 4.79 mm.

contrast to the violet sapphire host. As a composite of hydrated iron oxide minerals, the limonite's yellow color is a strong indication that the stone has not been heat treated, as this would cause the yellow limonite to alter into red hematite (J.I. Koivula, "Useful visual clue indicating corundum heat treatment," Fall 2013 *G&G*, pp. 160–161). This example demonstrates that even the most common of inclusions can occasionally materialize as something remarkable.

*Britni LeCroy and Nathan Renfro
GIA, Carlsbad*

Parasite Channels in a Saltwater Natural Pearl

Shell-boring parasitic worms are commonly found inside the shells of various pearl-producing mollusk species. Consequently, mollusk shells may exhibit elongated channels indicating the presence of such organisms. Recently, the author observed interesting parasite channel features inside an 8.25 mm natural saltwater pearl (figure 10) set in a brooch with other pearls and near-colorless stones.

Microscopic examination revealed a Y-shaped channel with numerous finer branches that likely formed as the parasite searched for a way out of the pearl. The channel opening was observed at the surface of the nacre, while the tunnel was located slightly beneath the nacre. This interesting feature matched the pearl's internal structure, with a similarly Y-shaped structure visible in the X-ray image. Although such channels are often found in shells, they are rarer in pearls, and this channel's unique shape and morphology are noteworthy.

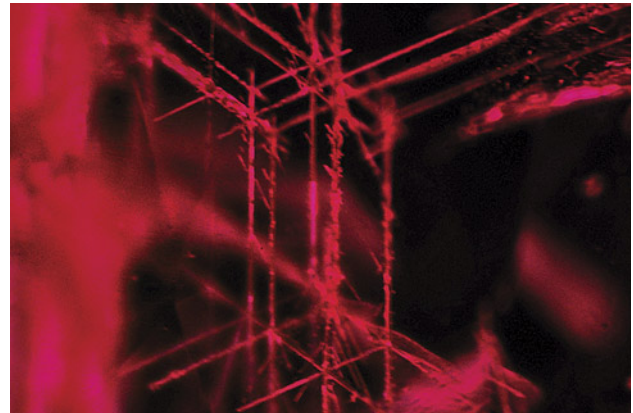
*Emiko Yazawa
GIA, New York*

Rose Channels in Ruby

The author recently examined a 0.5 ct pear-shaped ruby measuring 6 × 4 mm that contained twinning planes and hollow channels known as Rose channels (figure 11). Because the Rose channels were hollow and empty, they had a refractive index of 1 (the RI of air), while the RI of the surrounding host ruby was 1.76–1.77. The contrasting refractive indices resulted in high optical relief, making the Rose channels easily visible. These linear inclusions are common in natural corundum and were once thought to be boehmite needles (F. Notari et al., "Boehmite needles' in corundum are Rose channels," Fall 2018 *G&G*, p. 257).

*Aamir Sayed
Al Zain Jewellery, Bahrain*

Figure 11. Rose channels in a 0.5 ct ruby. Photomicrograph by Aamir Sayed; field of view 0.75 mm.



“Cyber” Butterfly

The author recently examined a 2.56 ct purple octagonal step-cut sapphire. This sapphire contained a negative crystal with a sharp rectilinear zigzag-patterned fingerprint, providing strong evidence that no heat treatment took place. Under fiber-optic illumination, the fingerprint displayed vibrant colors due to thin-film interference. The combination of the fingerprint and negative crystal created an image reminiscent of a digital butterfly (figure 12). Both the negative crystal and the unique fingerprint were caused by the natural healing of a surface-reaching fracture in the sapphire host. The healed areas parallel to the *c*-axis displayed rectangular outlines, resulting in the “cyber” appearance of the wings.

Yuxiao Li
GIA, Tokyo

Tourmaline Inclusion with Included Crystals in Kashmir Sapphire

The authors recently examined a 1.81 ct blue cushion mixed cut identified as sapphire. Microscopic examination showed sharp-banded milky clouds, particle stringers, and a well-formed euhedral greenish crystal. The crystal displayed a triangular prismatic habit with sharp basal pinacoids. This is typical of tourmaline, and the inclusion's identity was later confirmed by Raman spectroscopy.

Tourmaline inclusions in sapphire are diagnostic of a Kashmir origin (see R. Schwieger, “Diagnostic features and

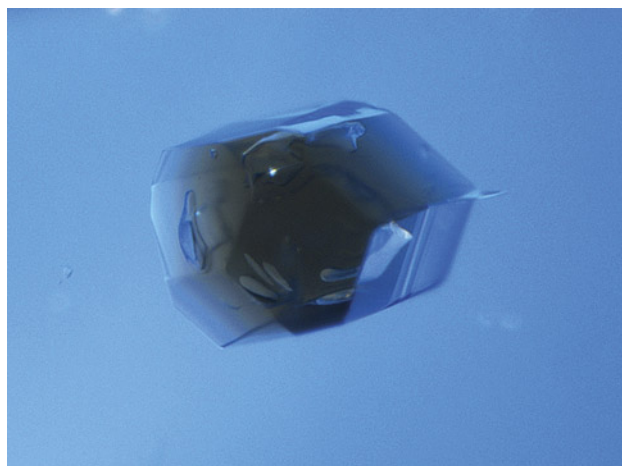


Figure 13. This tourmaline inclusion in a 1.81 ct Kashmir sapphire contains a few unusual “daughter” crystals with rounded edges. Photomicrograph by Yusuke Katsurada; field of view 0.73 mm.

heat treatment of Kashmir sapphires,” Winter 1990 *G&G*, pp. 267–280). Trace element analysis with laser ablation–inductively coupled plasma–mass spectrometry supported the microscopic observations, revealing a chemistry consistent with classic Kashmir samples from GIA’s colored stone reference collection.

Interestingly, the tourmaline possessed uneven rounded inclusions of its own (figure 13). These crystals were presumably a different material, given their lighter

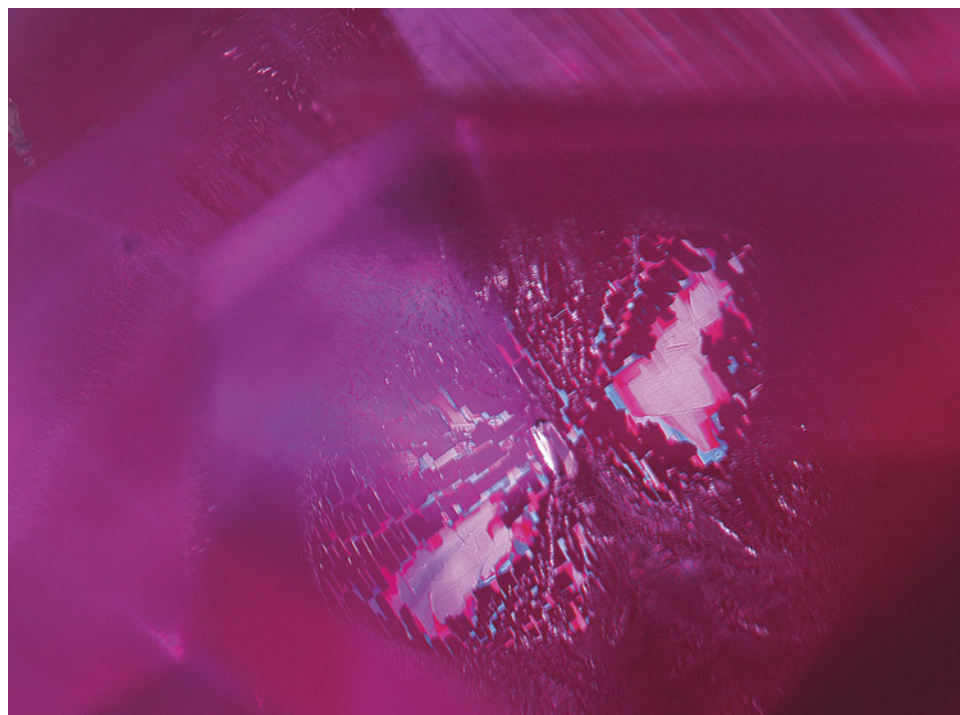


Figure 12. The rectilinear zigzag-patterned fingerprint and the negative crystal in the center are reminiscent of a beautiful “cyber” butterfly trapped in this 2.56 ct purple sapphire. Photomicrograph by Yuxiao Li; field of view 2.60 mm.

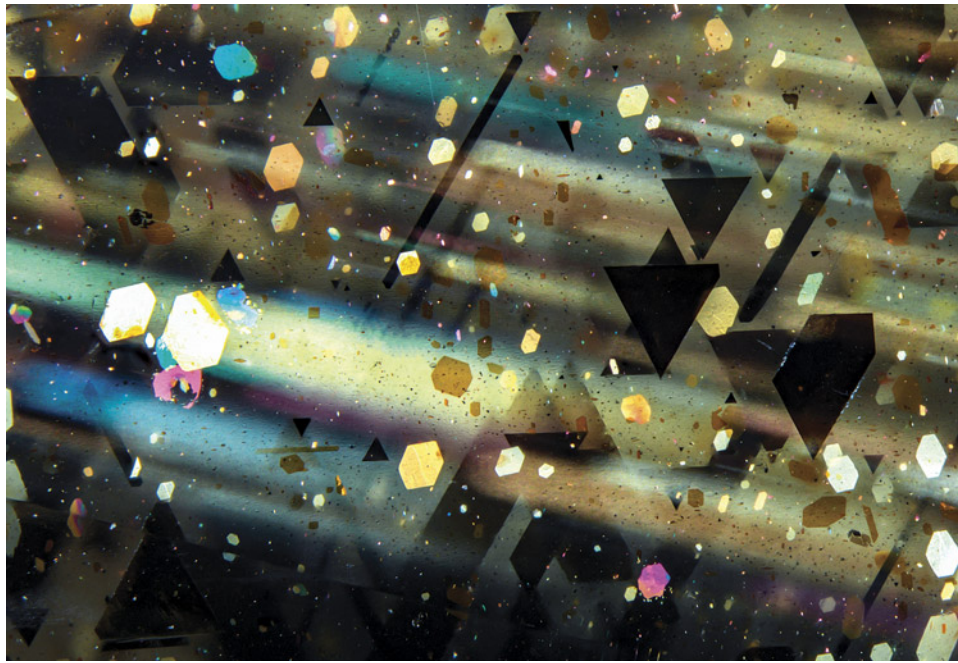


Figure 14. Parallel rays of golden, pink, and blue light were observed in this sample of rainbow lattice sunstone. Photomicrograph by Rosie Young; field of view 5.33 mm.

tone and sharp boundaries, which contrasted with the tourmaline host. Unfortunately, they could not be identified with Raman spectroscopy, leaving us to speculate about their true nature.

Yusuke Katsurada
GIA, Tokyo
Tyler Smith
GIA, New York

Rainbow Rays in Rainbow Lattice Sunstone

While examining a polished sample of Australian rainbow lattice sunstone, the author noticed a series of parallel

“rays” illuminated with fiber-optic lighting (figure 14). These rays were initially considered some kind of internal structure within the feldspar. However, the orientation of the rays changed direction when the stone was tilted (figure 15). This indicated an optical effect whereby the fiber-optic light reflected off hematite inclusions and produced a ray of light corresponding to the color of the hematite platelet. This can be observed most easily in the upper right corner of figure 14. Extremely small particles within the sunstone likely allow the path of light to be visible, much like headlights shining through fog.

Rosie Young
Gemmological Certification Services, London

Figure 15. The changing direction of the rays is visible here when the stone is viewed through the same polished face but tilted to a slightly different orientation. Photomicrographs by Rosie Young; field of view 19.27 mm.



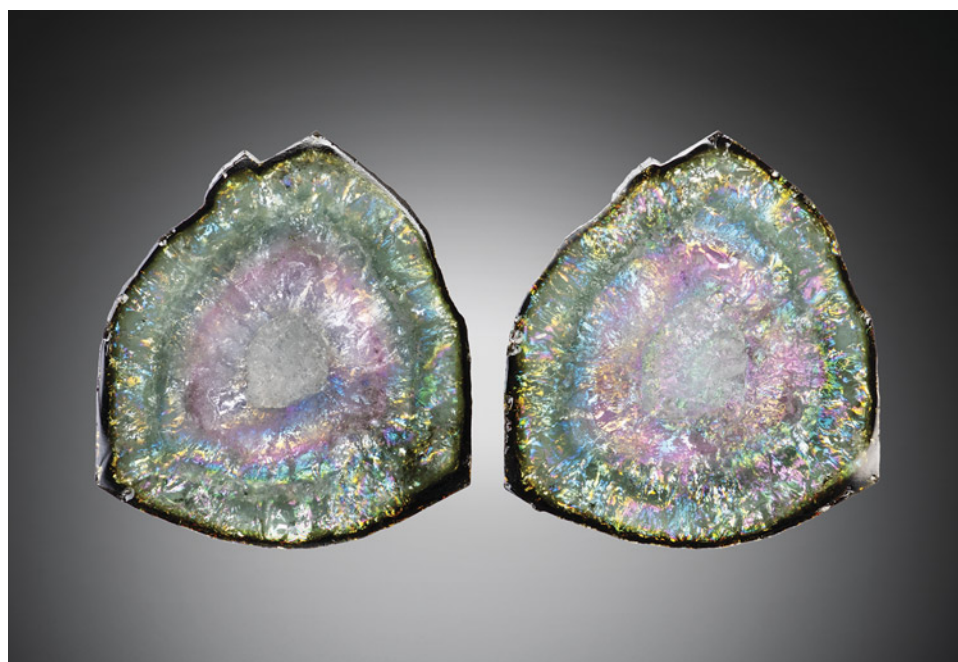


Figure 16. These 18 × 18 × 4 mm watermelon tourmaline slices (17.82 ct on the left and 17.17 ct on the right) display an exceptional iris effect. Photo by Jeffrey Scovil.

Brazilian Watermelon Tourmaline with Iris Effect

The watermelon tourmaline slices shown in figure 16 are remarkable for their mesmerizing iris effect. Unearthed from the famed Cruzeiro mine in the Brazilian state of Minas Gerais more than seven years ago, they were precisely cut to unveil their rainbow spectrum. Each slice, measuring 18 × 18 × 4 mm, radiates an alluring interplay of colors attributed to the iris effect, a phenomenon created by subtle internal fractures within the gemstone. This rare flawlessly matched pair weighed 34.99 carats total, conjuring the enchantment of fiery Australian opals.

*Russ Behnke
Meriden, Connecticut*

Quarterly Crystal: Diamond in Diamond

Mineral inclusions in diamonds are always very interesting to gemologists and other geoscientists, and the colorful minerals such as bright green chromium diopside and orange almandine-pyropo usually attract the most attention. This Quarterly Crystal is slightly different, in that the inclusion is both transparent and colorless, with relatively low relief compared to the diamond crystal host. The parent diamond, a transparent colorless, gem-quality glassy octahedron, weighed 0.71 ct and measured 5.88 × 3.99 × 3.01 mm (figure 17). Reportedly from South Africa, the diamond was purchased at the Tucson shows from David New.

Figure 17. With a weight of 0.71 ct and measuring 5.88 mm in longest dimension, this glassy colorless diamond octahedron contains an eye-visible diamond inclusion.

Photo by Diego Sanchez.

When inclusion-host pairs are composed of the same mineral, it causes a low-relief situation bordering on in-





Figure 18. Polarized light shows an elongated modified diamond octahedron displaying various degrees of interfacing with the host diamond crystal. Photomicrograph by Nathan Renfro; field of view 2.18 mm.

visibility. Such inclusions become visible when the orientation of the inclusion is different or when there is an interface or partial interface between the host and the inclusion. In the case of diamond in diamond, if the inclusion is visible, then the interface can consist of various fluids and gases, other minerals (most commonly graphite formed through graphitization), combinations of all of these, or nothing at all.

Examining the outline of the diamond inclusion in figure 18, there are areas at the interface where the inclusion and host diamond appear to blend perfectly and the interface seems to completely disappear. These are areas of perfect contact where the diamond inclusion and the diamond host merge, without any form of interfacial separation.

*John I. Koivula and Nathan Renfro
GIA, Carlsbad*

